Estimation of Composite Daylight-Fluorescent Light Components Based on Multi-spectral Scene Images

Shoji Tominaga, Department of Engineering Informatics, Osaka Electro-Communication University, Neyagawa, Osaka 572-8530, Japan

Abstract

A solution method is proposed for the illuminant estimation problem in the case of composite illuminants involving both spiky and continuous spectra. A spectral imaging system is utilized for image acquisition and analysis of scene reflections under spiky-spectrum illuminants. Fluorescent illuminants can be classified into three groups based on a set of wavelengths of the line spectra. Therefore we can infer the material classes of fluorescent light sources by estimating the wavelength positions of spikes on the illuminant spectrum. An estimation procedure is comprised of two major steps: First, the fluorescent illuminant class is determined from the multi-spectral images of a scene. Second, the spectral distributions of the illuminant components of fluorescent light and daylight are estimated based on an extended linear model. The feasibility of the proposed method is examined on natural scene reflections occurring under spiky fluorescent light and continuous daylight.

Introduction

The use of fluorescent light sources has been steadily increasing for indoor lighting and street lighting, because they are more efficient, luminous, and have a longer life than incandescent lamps. Under these circumstances, we note that the ambient illumination often is a compound of fluorescence and daylight (or incandescent light). That is, the ambient illuminant spectrum consists of the sum of the spiky fluorescent spectrum and the continuous daylight spectrum. Therefore we pose a new illuminant estimation problem: Estimation of light source components from image data of natural scenes. However, it is clear that the usual RGB camera systems are inappropriate for solving this image acquisition and estimation problem.

The present paper proposes a solution method for the illuminant estimation problem in the case of composite illuminants involving both spiky and continuous spectra. A spectral imaging system with narrow band filtration is utilized for image acquisition and analysis of scene reflections under spiky-spectrum illuminants. We note that the characteristic wavelengths of the line spectra are inherent to the fluorescent materials of the light source, and the number of fluorescent illuminants is limited. Our preliminary studies [2-3] show that fluorescent illuminants can be classified into three groups based on a set of wavelengths of the line spectra. Therefore we can infer the material classes of fluorescent light sources by estimating the wavelength positions of spikes on the illuminant spectrum.

An effective procedure for scene illuminant estimation is comprised of two major steps: In the first step the fluorescent illuminant class is determined from the multi-spectral images of a scene. In the second step the spectral distribution of the illuminant components of fluorescent light and daylight are estimated. The feasibility of the proposed method is demonstrated in experiments conducted on natural scene reflections occurring under spiky fluorescent light and continuous daylight.

Spectral Imaging System

We realize a spectral imaging system using a liquid-crystal tunable (LCT) filter, a monochrome CCD camera, and a personal computer. Figure 1 shows the camera system. The LCT filter operates over the visible wavelength range [400-700 nm], and the bandwidths are about 20 nm. The camera is a scientific camera with a cooling system to reduce noise. The present camera is the Qimaging-model RETIGA 1300C, which utilizes Peltier cooling. The bit depth of the image is 12 bits.

We sample the range [400-700 nm] at intervals of 5 nm and acquire the monochrome images at 61 wavelengths. Moreover we acquire additional images at eight wavelengths of 404, 436, 488, 544, 580, 588, 612, and 656 nm that correspond to bright line spectra of main fluorescent lamps. Figure 2 shows the overall spectral-sensitivity functions, which are determined as a combination of the spectral-sensitivity functions of the monochrome camera and the spectral transmittances of the LCT filter. Each spectral curve is normalized as a unit length vector. The red bold curves in Figure 2 represent the additional sensor responses. Therefore, the spectral image consisting of a set of 69 monochrome images is acquired for one shot of a natural scene. We have realized a computer control system for automatically acquiring a set of spectral images.
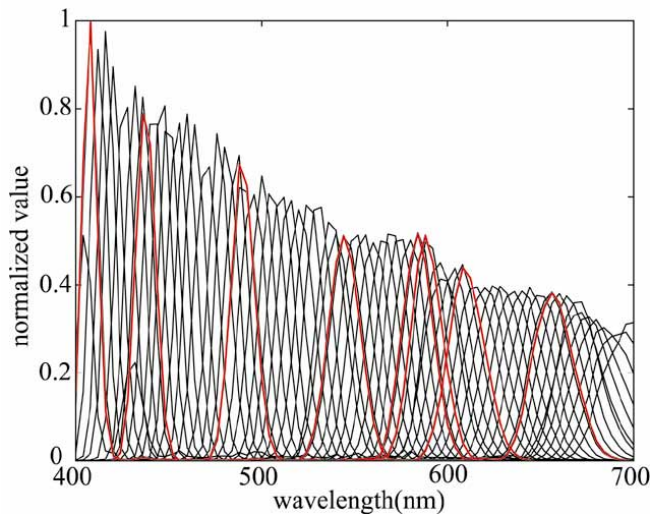

Figure 1. Spectral camera system.

Figure 2. Overall spectral-sensitivity functions.

Figure 3. Typical fluorescent spectral curve.

Characteristics of Fluorescent Spectra

Figure 3 shows a typical spectral curve of fluorescent illuminants. The spectral curve is divided into several peak areas and a background continuum. The spike peaks are considered as the significant feature of a fluorescent spectral distribution. The wavelength coordinates of the peaks correspond to the energy levels emitting fluorescence, which are inherent to the fluorescent material itself. Therefore a set of the peak wavelengths provides us a key to identifying the unknown fluorescent light source when we observe scene illumination.

A database of fluorescent light sources is used for analysing the spectral features. Our database consists of 18 different spectra from the CIE fluorescent lamps and real fluorescent lamps. The CIE defined spectral power distributions representing typical fluorescent lamps [3], which are twelve light sources F1, F2, …, F12, including daylight fluorescence, cool white fluorescence, and three narrow-band fluorescence. In addition, we collected ten real fluorescent lamps from products on the market. These fluorescent lamps are White W/M/36, Museum (daylight), Museum (bulb), Test Color D65, Mellow 5D, Meat Display, Mellow 5D-Ball, PA-Look Ball EFG13EL, PA-Look Ball EFG13ED, and F10-TL84. The spectral-power distributions were measured using a spectro-radiometer.

We investigated sharp and big peaks on the respective fluorescence-spectral distributions in the database. It is found that all the fluorescent spectral curves can be classified into three groups based on the wavelengths of spike peaks as shown in Figure 4. The first group that we call the "Standard" type has the main peaks at 436, 544, and 580 nm, which includes CIE-F1, …, CIE-F9, White W/M/36, Museum (daylight), and Test Color D65. The second group called the "Three narrow-band" type has the main peaks at 436, 488, 544, and 612 nm, which includes CIE-F10, CIE-F11, CIE-F12, and Mellow 5D. The third group called
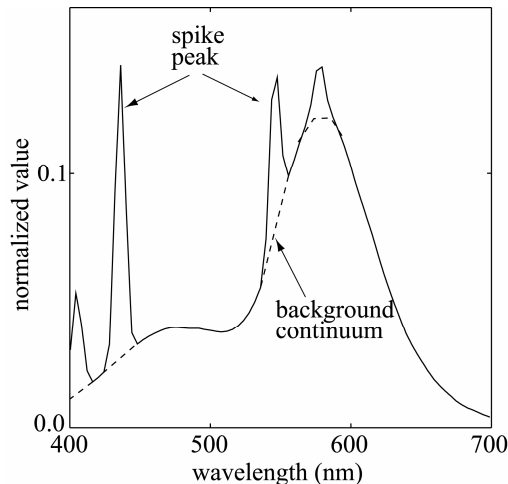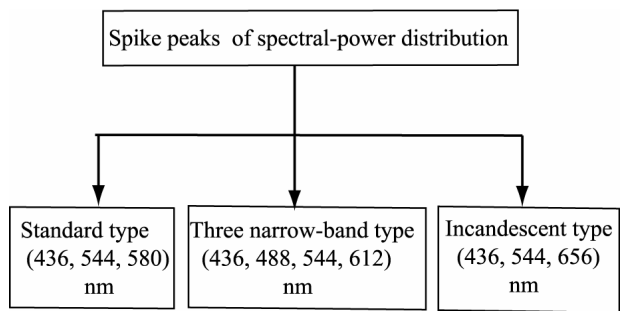

Figure 4. Three types of fluorescent spectra.

the "Incandescent" type has the main peaks at 436, 544, and 656 nm. This group includes Museum (bulb) and Meet display.

Detection of Fluorescent Component

We adopt the gray world assumption for the purpose of illuminant estimation. It assumes that the average of surface reflectances over the entire scene is gray. Let $\rho_k(x)$ ($k = 1, 2, …, f$) be the camera outputs at spatial location x with f wavelength bands λ_1, λ_2, …, λ_f. Under the narrow band assumption to each sensor, the spctral radiance at location x is described in the form

$$Y(\lambda_k, x) = \rho_k(x) \Big/ \int_{380}^{720} R_k(\lambda) d\lambda , \qquad (k = 1, 2, …, f) \qquad (1)$$

where $R_k(\lambda)$ is the spectral sensitivity function of the k-th channel. Therefore the illuminant spectra $E(\lambda)$ is estimated as the average spectral radiance $E(\lambda_k) = \mathrm{E}\{Y(\lambda_k)\}$ over the entire location x.

The fluorescent peaks are detected using the average spectral radiance $\mathrm{E}\{Y(\lambda_k)\}$ ($k=1, 2, …, f$). However the average spectral curve does not necessarily have sharp peaks because the spectral sensitivity functions of the spectral camera are not ideal narrow bands, and the average operation is performed for the entire image including a variety of objects in a scene. Figure 5 illustrates a simulation result using the Macbeth Color Checker and a fluorescent lamp of the incandescent type. The bold curve shows

the average spectral camera outputs $E\{Y(\lambda_k)\}$ (k=1, 2, …, 69). The broken curve in the figure shows the real spectral curve of the incandescent type lamp, which was measured directly by a spectro-radiometer and a standard white reference. Peaks on the average spectral curve are not coincident with the original fluorescent peaks.

We propose to take the derivative of the camera output spectra for detecting "slow" changes on the spectral curves. The first derivative called the gradient calculates a slope of spectrum at each channel wavelength. The second derivative called the Laplacian calculates the divergence of the gradient of a spectral curve. We define the operation as

$$X''(\lambda_k) = -(X'(\lambda_{k+1}) - X'(\lambda_{k-1}))/(\lambda_{k+1} - \lambda_{k-1}) . \quad (2)$$

Figure 6 shows an example for the derivative of the Gauss function. The Laplacian operation is effective for peak detection. Thus the problem of finding spike peaks on the observed illuminant spectrum is reduced to the problem of detecting peaks of the second derivative spectrum.
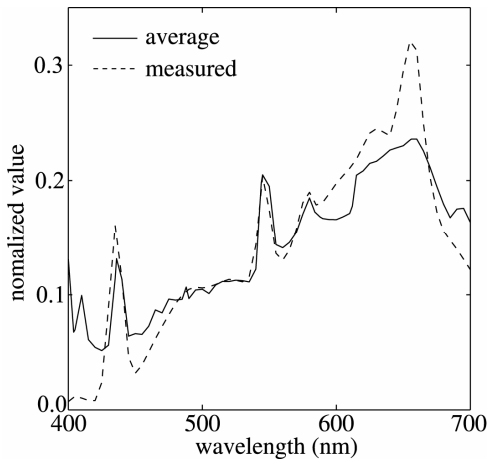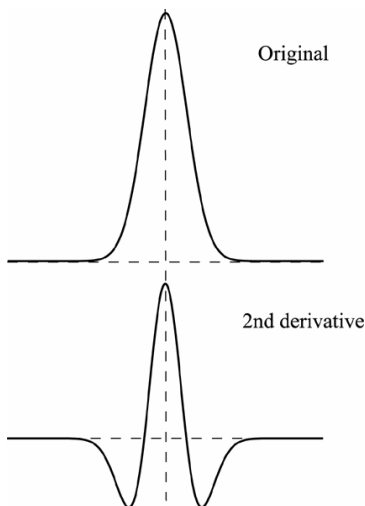

Figure 5. Example of average sensor outputs.

Figure 6. Derivative for the Gauss function.

Estimation of Composite Illuminant Components

Suppose that the ambient illuminant in a natural scene is a compound of fluorescent and daylight (or incandescent light). Let $F_0(\lambda)$ and $K(\lambda)$ be the spiky fluorescent spectrum and the continuous daylight spectrum, respectively. Then the spectral-power distribution of the ambient light is described as a linear combination

$$E(\lambda) = \alpha F_0(\lambda) + \beta K(\lambda) , \quad (3)$$

where α and β are weighting coefficients representing the intensities of the light sources.

First, we determine the fluorescent illuminant class by the above peak detection method for the observed spectrum. The light sources in each class are considered to have the same fluorescent materials, so that the spectral curves are close each other in the same class. Figure 7 shows the average fluorescent illuminant spectra representing the three types of the Standard, the Three-narrow band, and the Incandescent.

Next, we describe the unknown continuous spectrum $K(\lambda)$ by using the finite-dimensional linear model. The illuminant spectrum is then expressed in a linear combination of three basis functions. To derive the basis functions, we used a set of measured spectra from the CIE standard lights and several real sources. Figure 8 shows the basis functions used in this study, which were obtained as the first three principal components of the set of illuminant spectra. Therefore the ambient illuminant is represented as an extended linear model

$$E(\lambda) = \alpha F_0(\lambda) + \varepsilon_1 E_1(\lambda) + \varepsilon_2 E_2(\lambda) + \varepsilon_3 E_3(\lambda) , \quad (4)$$

where { ε_i } is a set of weights for the basis functions.

Substituting (4) into the camera equation leads to the multi-band camera outputs in a matrix form as

$$\Delta = \begin{bmatrix} \rho_1 \\ \rho_2 \\ \vdots \\ \rho_f \end{bmatrix} = \begin{bmatrix} \mathbf{R}_1^t \\ \mathbf{R}_2^t \\ \vdots \\ \mathbf{R}_f^t \end{bmatrix} \begin{bmatrix} \mathbf{F}_0 , \mathbf{E}_1 , \mathbf{E}_2 , \mathbf{E}_3 \end{bmatrix} \begin{bmatrix} \alpha \\ \varepsilon_1 \\ \varepsilon_2 \\ \varepsilon_3 \end{bmatrix}$$

$$(5)$$

where { $\mathbf{R}_i$ } are a set of n-dimensional vectors representing the camera spectral sensitivities and { $\mathbf{F}_0 , \mathbf{E}_1 , \mathbf{E}_2 , \mathbf{E}_3$ } are a set of vectors representing the average spectral function and the basis functions. The symbol t stands for matrix transposition. In practical numerical computation, all spectral curves are sampled at 5nm intervals in the range [380, 720nm].

Thus the problem of estimating the composite illuminant components can be reduced to solving the four-dimensional linear model. Since the camera spectral sensitivity functions, the average spectral functions of the three fluorescent types, and the basis functions of continuous illuminants are known in advance, the weighting coefficients α, ε_1, ε_2, and ε_3 are estimated from
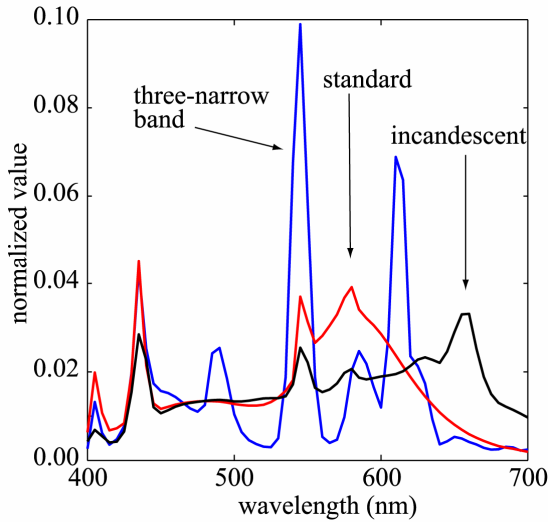
Figure 7. Average fluorescent spectra for three types.

Figure 9. Objects used in experiments.
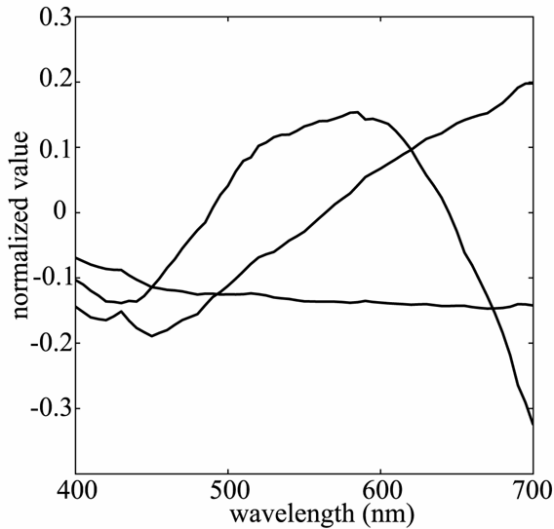
Figure 8. Basis functions for continuous illuminant spectra.

Figure 10. Illumination from fluorescent ceiling lamps and daylight through a window.

the multi-band camera outputs based on the standard least-squared method.

Experiments

We have examined the proposed method for estimating composite illuminant components of spiky fluorescent light and continuous light based on the multi-band camera images. We use eight real fluorescent lamps for the spiky spectral sources, and used daylight coming through a window and an incandescent lamp for the continuous spectral sources. The objects are dolls and toys as shown in Figure 9, which are made of plastic and painted clay. Figure 10 shows the scene in an experimental room where the objects on a table are illuminated with both fluorescent ceiling lamps and daylight through the window. The camera system was placed about 150cm apart from the objects and at the same height.

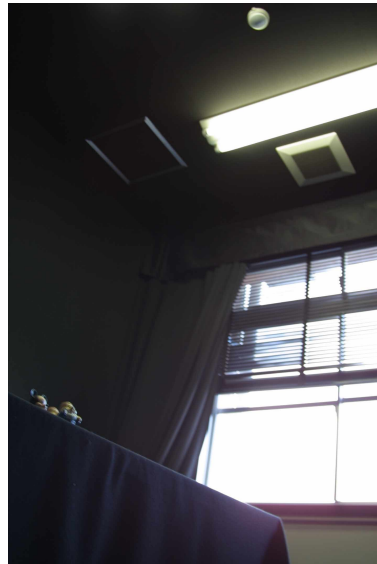Let us first show the results for use of the Standard type of fluorescent light. Figure 11 depicts the spectral-power distribution measured for the composite spectrum of a White W/M/36 fluorescent lamp and the daylight. Figure 12 depicts the camera outputs with 69 channels at all pixels of the scene image. We calculated the second derivative of the output spectra at all pixels, and then calculated the average of the second derivatives over the pixels. This calculation should provide the same answer as the calculation of the second derivative for the average spectral outputs. In practical numerical computation, however, the present calculation provides more effectively spike peaks on the second derivative curve. Figure 13 shows the average second derivative curve. We can see three main peaks at 436, 544, and 580 nm, so that the fluorescent illuminant is classified into the Standard type. The red broken curve in Figure 13 shows the direct measurement of spectral-power distribution for the White W/M/36 lamp used. Next the composite illuminant components were estimated using
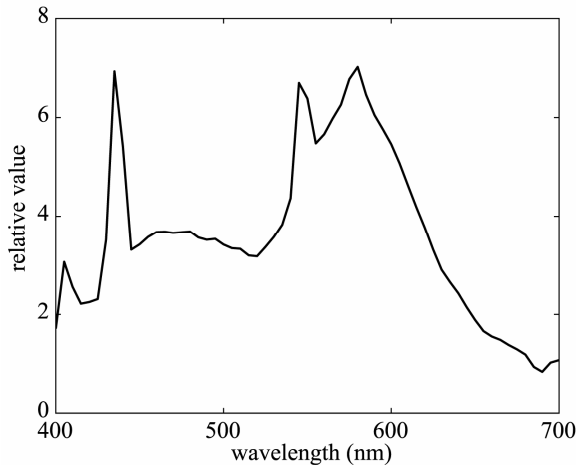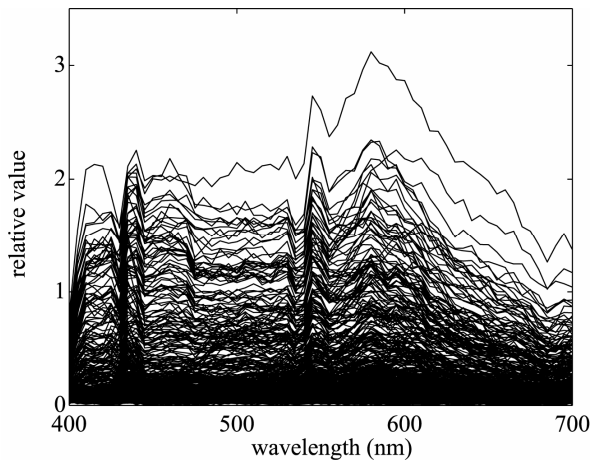
Figure 11. Composite spectral-power distribution.

Figure 12. All spectral camera outputs.

Figure 13. Average second derivative curve.

Figure 14. Estimation result of daylight spectrum.

the average fluorescent spectrum of the Standard type and three basis functions. The weighting coefficients of the linear model

were determined from the average data of the camera outputs. The continuous illuminant spectrum is then recovered from the estimated coefficients ε_1, ε_2, and ε_3. Figure 14 shows the estimation result of daylight spectrum. The red broken curve is the direct measurement by a spectro-radiometer.

Conclusion

This paper has proposed a solution method for the illuminant estimation problem in the case of composite illuminants involving both spiky and continuous spectra. A spectral imaging system with narrow band filtration was utilized for image acquisition and analysis of scene reflections under spiky-spectrum illuminants. Fluorescent illuminants can be classified into three groups based on a set of wavelengths of the line spectra. Therefore we can infer the material classes of fluorescent light sources by estimating the wavelength positions of spikes on the illuminant spectrum. We have presented an effective procedure for scene illuminant estimation in two major steps. First, the fluorescent illuminant
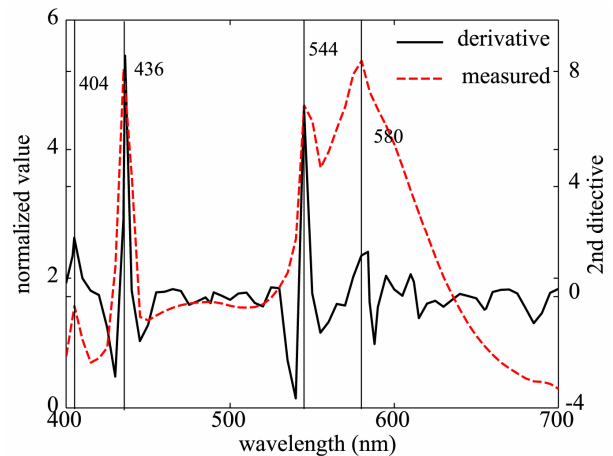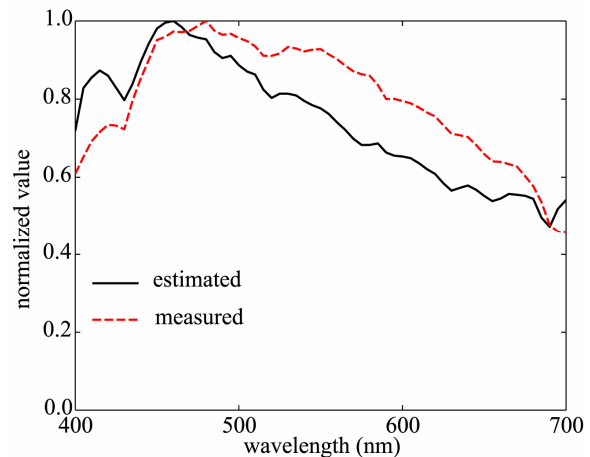
class was determined from the multi-spectral images of a scene. Second, the spectral distribution of the illuminant components of fluorescent light and daylight were estimated. The feasibility of the proposed method was demonstrated in experiments using reflective objects under fluorescent ceiling lamps and daylight through a window

References

[1] B.A. Wandell. Foundations of Vision, Sinauer Associates, Sunderland, MA, 1995.

[2] S. Tominaga and H. Haraguchi: Estimation of fluorescent scene illuminant by a spectral camera system, Proc. of SPIE, Color Imaging X, Vol. 5667, pp.128-135, San Jose, 2005.

[3] S. Tominaga and H. Haraguchi: A spectral imaging method for classifying fluorescent scene illuminant, Proc.of 10th Congress of the International Colour Association, pp.193-196, Granada, Spain, 2005.

[4] CIE: Colorimetry, Publication CIE No 15.2, 1986.

Author Biography

Shoji Tominaga was born in Hyogo Prefecture, Japan, 1947. He received the B.E., M.S., and Ph.D. degrees in electrical engineering from Osaka University, Japan, in 1970, 1972, and 1975, respectively. Since 1976, he has been with Osaka Electro-Communication University, Neyagawa,

Osaka, where he is currently Professor of Department of Engineering Informatics, and the chairman of Visual Information Research Institute. His research interests include color image synthesis/analysis and multi-spectral imaging. He is a Fellow of IEEE and a member of IS&T, SID, ACM, SPIE and OSA.